**Applied Energy Symposium 2020: Low carbon cities and urban energy systems**
**October 10-17, 2020**
**Paper ID: CUE 2020-D-032**

# Theory-guided LSTM for Day-ahead Forecasting of Photovoltaic Power Generation

Xing Luo[1, 2], Dongxiao Zhang[3, 1*], Xu Zhu[2, 4]

1 Intelligent Energy Lab, Peng Cheng Laboratory, Shenzhen, 518055, P. R. China

2 School of Electronic and Information Engineering, Harbin Institute of Technology, Shenzhen, 518055, P. R. China

3 School of Environmental Science and Engineering, Southern University of Science and Technology, Shenzhen, 518055, P. R. China

4 Department of Electrical Engineering and Electronics, University of Liverpool, Liverpool, L69 3GJ, U.K

**ABSTRACT**

This paper considers domain knowledge of photovoltaic (PV) and proposes a theory-guided long-short-term memory (Tg-LSTM) framework to forecast the hourly day-ahead PV power generation (PVPG). It aims to overcome the shortcoming of recent machine learning algorithms that are applied based only on massive data, and are thus easily producing unreasonable forecasts. Real-life PV datasets are adopted to evaluate the feasibility and effectiveness of the models. The results indicate that the proposed Tg-LSTM model possesses stronger forecasting capability than the standard LSTM model. It is more robust against PVPG forecasting, and more suitable for PVPG forecasting with sparse data in practice. The Tg-LSTM model also demonstrates superior performance with higher accuracy of PVPG forecasting compared to conventional machine learning methods.

**Keywords:** solar energy, forecasting, domain knowledge, theory-guided LSTM

## 1. INTRODUCTION

Accurate forecasting of photovoltaic power generation (PVPG) is extremely important, as it can constitute a decision-making tool in power system operations [1]. Indeed, it is beneficial for both power suppliers and power systems. Power suppliers need to obtain precise information about PVPG for setting up dedicated commercial offers, thus reducing production cost and increasing profit. Meanwhile, it can also mitigate the negative impact caused by PV power uncertainty, ensuring the stability and reliability of the power system [2]. However, the PV output of a system mainly depends on the intensity of solar irradiance and a variety of meteorological factors, which are usually both uncertain and ungovernable [3]. The power generation of a PV system varies dynamically with time due to the variability of meteorological factors. Therefore, an accurate and stable forecasting of PVPG is considerably difficult and remains challenging.

In recent years, the latest development of smart metering technologies has given rise to an enormous volume of data, which is beneficial for the evolution of machine learning (ML) models. ML models (e.g., LSTM [1]) have become the most frequently used method in practice [4]. Despite numerous successes obtained from previous works, limitations remain in PVPG forecasting. The research gaps can be generally summarized as: (1) Recent ML models are applied based only on massive data, and thus easily produce physically unreasonable forecasts. No domain knowledge or physical laws are involved in the construction of the model. (2) A large amount of data is usually required to guarantee model accuracy, whereas data collection is both time-consuming and expensive. ML models may exhibit low performance without sufficient data.

To overcome the above constraints, incorporating domain knowledge and physical laws of PV, a deep learning based framework, the so-called theory-guided LSTM (Tg-LSTM), is proposed in this work, to forecast hourly day-ahead PVPG. The main contributions of our work are summarized as follows: (1) Constraints are extracted from domain knowledge of PV, and then firstly

Selection and peer-review under responsibility of the scientific committee of CUE2020

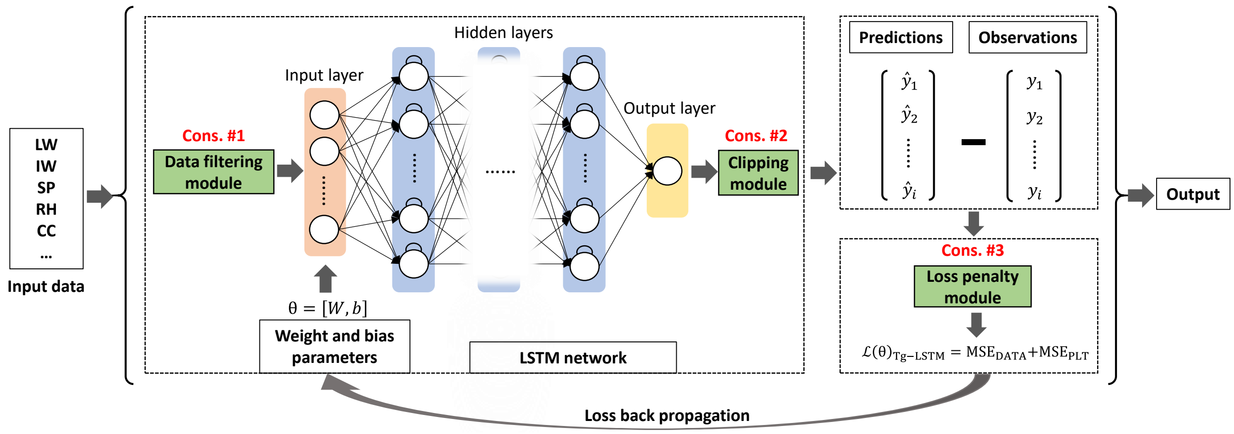


Fig. 1: Architecture of the Tg-LSTM model with three constraint modules.

integrated into the construction of the Tg-LSTM model. (2) The Tg-LSTM model is more robust against PVPG forecasting, and more suitable for PVPG forecasting with sparse data than the standard LSTM model in practice. (3) The Tg-LSTM model can achieve better performance with higher accuracy of PVPG forecasting compared to conventional ML methods.

The remainder of this paper is organized as follows. In Section 2, the proposed Tg-LSTM model is illustrated specifically. After that, the Tg-LSTM model is evaluated based on real-life PV datasets in Section 3. The forecasting performances of different models are also compared. Finally, the paper is concluded in Section 4.

## 2. THEORY-GUIDED LSTM MODEL

The Tg-LSTM model is developed based on the standard LSTM [1]. For the standard LSTM, it may produce physically unreasonable predictions for PVPG in training and testing processes (e.g., negative power generation, positive power generation at midnight, low solar radiation predicting high power generation, and high solar radiation predicting extremely low power generation) [1, 5]. This may occur in a deep neural network without incorporating domain knowledge and physical laws [6]. In this section, several constraints are extracted from domain knowledge of PV at first, and then integrated into the construction of the Tg-LSTM model. It aims to overcome the shortcoming of recent machine learning algorithms that are applied based only on massive data without considering the impacts of physical regulations on the model. The architecture of the Tg-LSTM model is presented in Fig. 1. In this work, three types of constraints (indicated as Cons. #1, Cons. #2, and Cons. #3 in Fig. 1) are integrated into the construction of Tg-LSTM.

### *2.1 Data filtering module*

The first module is called the ***Data Filtering Module***, which filters the input data into different periods of time according to a flag variable. It is designed based on world knowledge or general knowledge of PV [7], and aims to eliminate physically unreasonable forecasts, such as positive power generation at midnight, via filtering training data.

As discussed in Section 1, PV power production is significantly dependent on the solar radiation received by the PV panels near the land surface. Consequently, it is important to flag periods that have positive solar radiation at the surface. This is accomplished automatically by the data filtering module based on values of the time series variable, termed hourly surface radiation ($\mathrm{SR}^*$). In the training stage, only the data in flagged periods can be transferred into the model for further training and used to forecast the PV output. On the other hand, in the forecasting stage, for periods when the surface radiation is expected to be zero, the resulting PV output will be calculated accordingly. Due to less data being adopted for model training, the efficiency of Tg-LSTM can be improved to a certain degree.

### *2.2 Clipping module*

The second constraint integrated into the Tg-LSTM is called the ***Clipping Module***, which is used to restrict the output of the model in both training and testing processes. It is designed based on natural science knowledge of PV [7], and aims to eliminate physically unreasonable forecasts, such as negative power generation. According to the physical law, the value of PVPG should be physically greater than zero in practice, and therefore the model output should be positive. As a result, the output of Tg-LSTM, $\hat{y}_i$, should be subject to the constraint in Eq. (1).

$$\hat{y}_i \coloneqq \mathrm{ReLU}\big(NN(x_i;\theta)\big) \tag{1}$$

where $\mathrm{ReLU}(\cdot)$ is the rectified linear unit function. The ReLU function returns zero when the input to the function is negative, and returns the original value of the input when it is positive.

### *2.3 Loss penalty module*

Engineering controls in practice may also assist to guide the construction of Tg-LSTM. As PV power is converted directly from surface radiation, the amount of PVPG for a certain period of time should theoretically fall into a certain range while the amount of solar radiation is determined. According to the photoelectric conversion relationship between $\mathrm{SR}^*$ and PVPG, as illustrated in Fig. 2, the PV power output should fall within certain bounds, which may be constructed with historical data or on theoretical grounds. The outliers, marked as black crosses in the figure, can be detected by using the K-means algorithm [8] based on a proper evaluation criterion.

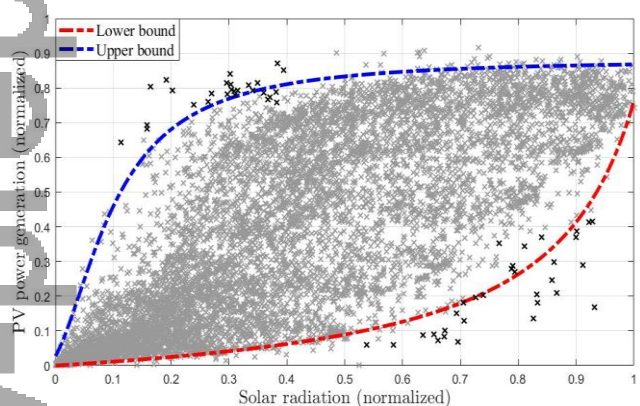


Fig. 2: Photoelectric conversion relationship between hourly solar radiation and PVPG of a typical PV plant.

Subsequently, the upper and lower bounds can be determined by bounding points among historical data. As a result, upper and lower bound functions are defined as bound controls to restrict the forecasts of PV output during the training process. In this study, the rational function is utilized to derive the lower and upper bound functions as $f^{\mathrm{LB}}(x)$ and $f^{\mathrm{UB}}(x)$, respectively. It is noted that the rational function is not the only format that can be used for the fitting task. Fitting functions in other formats, such as polynomial, exponential, and power with appropriate coefficients, are also acceptable.

Integration of the above constraint into the Tg-LSTM model is by reconstructing the loss function via the ***Loss Penalty Module***. Theoretically, when those bound controls are violated, there should be a penalty loss term or knowledge-based loss term $\mathrm{MSE}_{\mathrm{PLT}}$, reflected in the loss function [7]. Therefore, the loss function of the Tg-LSTM model can be reformulated as:

$$\mathcal{L}(\theta)_{\mathrm{Tg-LSTM}} = \mathrm{MSE}_{\mathrm{DATA}} + \mathrm{MSE}_{\mathrm{PLT}} \tag{2}$$

where

$$\mathrm{MSE}_{\mathrm{DATA}} = \frac{1}{N_{\mathrm{DATA}}}\sum_{i=1}^{N_{\mathrm{DATA}}} |\hat{y}_i - y_i|^2 \tag{3}$$

$$\mathrm{MSE}_{\mathrm{PLT}} = \frac{1}{N_{\mathrm{PLT}}}\sum_{i=1}^{N_{\mathrm{PLT}}} \lambda_{\mathrm{PLT},i}\cdot|\hat{y}_i - y_i^*|^2 \tag{4}$$

In Eq. (4), $\lambda_{\mathrm{PLT},i}$ is an additional hyper-parameter of Tg-LSTM, which denotes the intensity of penalty on the loss function, and $y_i^* = (f^{\mathrm{LB}}(x_i) + f^{\mathrm{UB}}(x_i))/2$. In the training process, when an output after the clipping module in the neural network, $\hat{y}_i$ (explained in Eq. (1)), satisfies the bound controls, $\lambda_{\mathrm{PLT},i} = 0$ and $\mathrm{MSE}_{\mathrm{PLT}} = 0$, this means that the model is trained as it used to be. In contrast, when the bound controls are violated, $\lambda_{\mathrm{PLT},i} > 0$ and $\mathrm{MSE}_{\mathrm{PLT}} > 0$, this indicates that additional penalties will be added to the loss function of Tg-LSTM. Meanwhile, the parameter vector $\theta = \{W, b\}$ will be tuned accordingly, and the model will be updated simultaneously. Therefore, $\lambda_{\mathrm{PLT},i}$ can be defined as follows:

$$\begin{cases} \lambda_{\mathrm{PLT},i} = 0,\ \hat{y}_i \in [f^{\mathrm{LB}}(x_i),\ f^{\mathrm{UB}}(x_i)] \\ \lambda_{\mathrm{PLT},i} > 0,\ \hat{y}_i \notin [f^{\mathrm{LB}}(x_i),\ f^{\mathrm{UB}}(x_i)] \end{cases} \tag{5}$$

The proposed constraint modules coordinate with each other to ensure that all outputs of the Tg-LSTM model are reasonable during training and testing processes.

## 3. CASE STUDY AND RESULTS

In Section 3, several case studies are carried out to evaluate the feasibility and effectiveness of the proposed methods. Real-life datasets of two typical PV plants are adopted.

### *3.1 Data preparation*

The feature dataset contains weather forecasts for 12 independent weather variables which are obtained from the European Center for Medium-range Weather Forecasts (ECMWF) [9] and five constructed weather variables. In the cross validation experiments, the

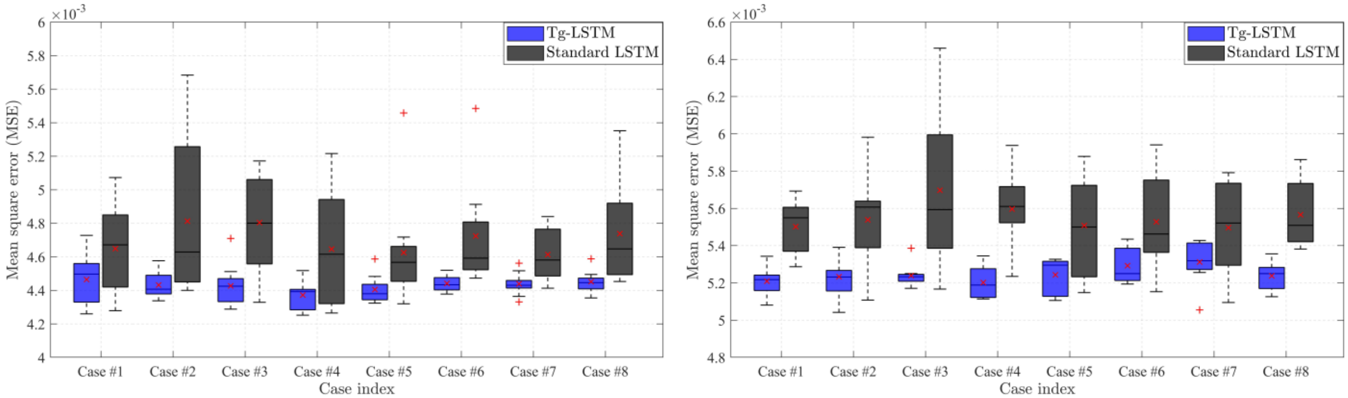


(a) (b)

Fig. 3: Robustness comparison between Tg-LSTM and LSTM models. (a) plant #1; (b) plant #2.

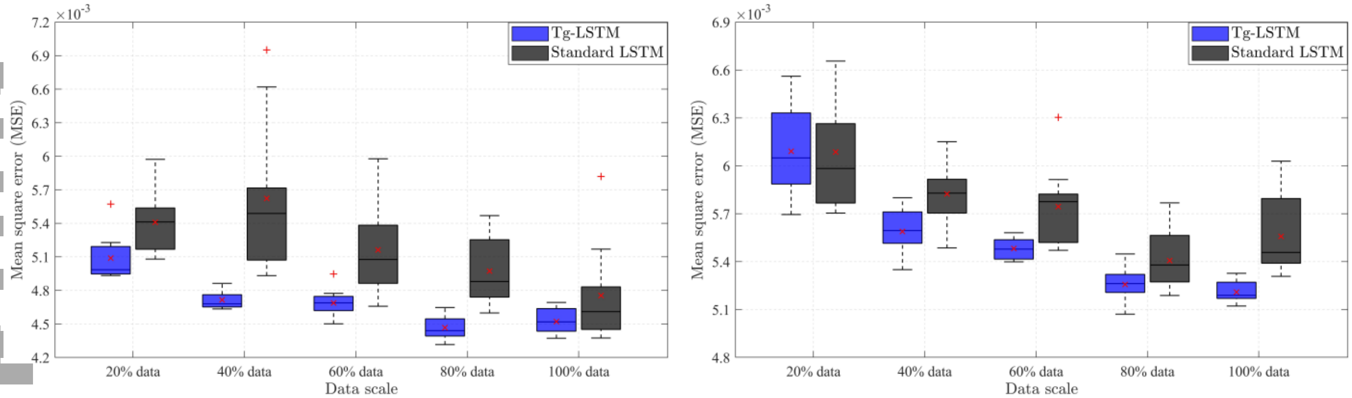


(a) (b)

Fig. 4: Comparison between Tg-LSTM and LSTM models based on different amounts of data. (a) plant #1; (b) plant #2.

historical data of 730 days (from 01-04-2012 to 31-03-2014, 2 years) are set as the training dataset, whereas the data of 91 days (from 01-04-2014 to 30-06-2014, 3 months) are set as the testing dataset to check over-fittings. Additionally, the min-max normalization, which restricts the data within the range between zero and one, is adopted. All feature data should be normalized prior to transmitting to the model. Several evaluation metrics including MAE, MSE, and $R^2$ score, are utilized to evaluate the forecasting performances.

### 3.2 *Forecasting capability of Tg-LSTM*

In this subsection, to compare the performance of the Tg-LSTM model versus the standard LSTM model, the forecasting capability of Tg-LSTM under different circumstances is evaluated. In all comparisons, the forecasting in night periods is not involved, and all programs have to be executed multiple times to reduce the impact of randomness.

Firstly, eight independent cases with different settings of hyper-parameters are utilized to evaluate the models in terms of robustness. For each case, the models are compared based on the same training data and hyper-parameters. Fig. 3 demonstrates the results of the robustness comparison between the standard LSTM and Tg-LSTM models for the two typical PV plants. From the results, it is obvious that the proposed Tg-LSTM model performs much better than the standard LSTM model, with higher accuracy and lower error STD in all cases. Therefore, the results indicate that the Tg-LSTM model is more robust against PVPG forecasting than the standard LSTM model.

Secondly, the forecasting performance of Tg-LSTM with sparse data is also evaluated. Different amounts (i.e., 20%, 40%, 60%, 80%, and 100%) of the training data from two typical PV plants are adopted to evaluate the forecasting capability of the Tg-LSTM model based on sparse data. From the results in Fig. 4, it can be seen that the forecasting error increases as the amount of adopted data decreases for both PV plants, in general, indicating the worth of data in Tg-LSTM. Compared to the standard LSTM model, the proposed Tg-LSTM model performs much better with lower MSE values, and the forecasting results of the Tg-LSTM model can still maintain relatively

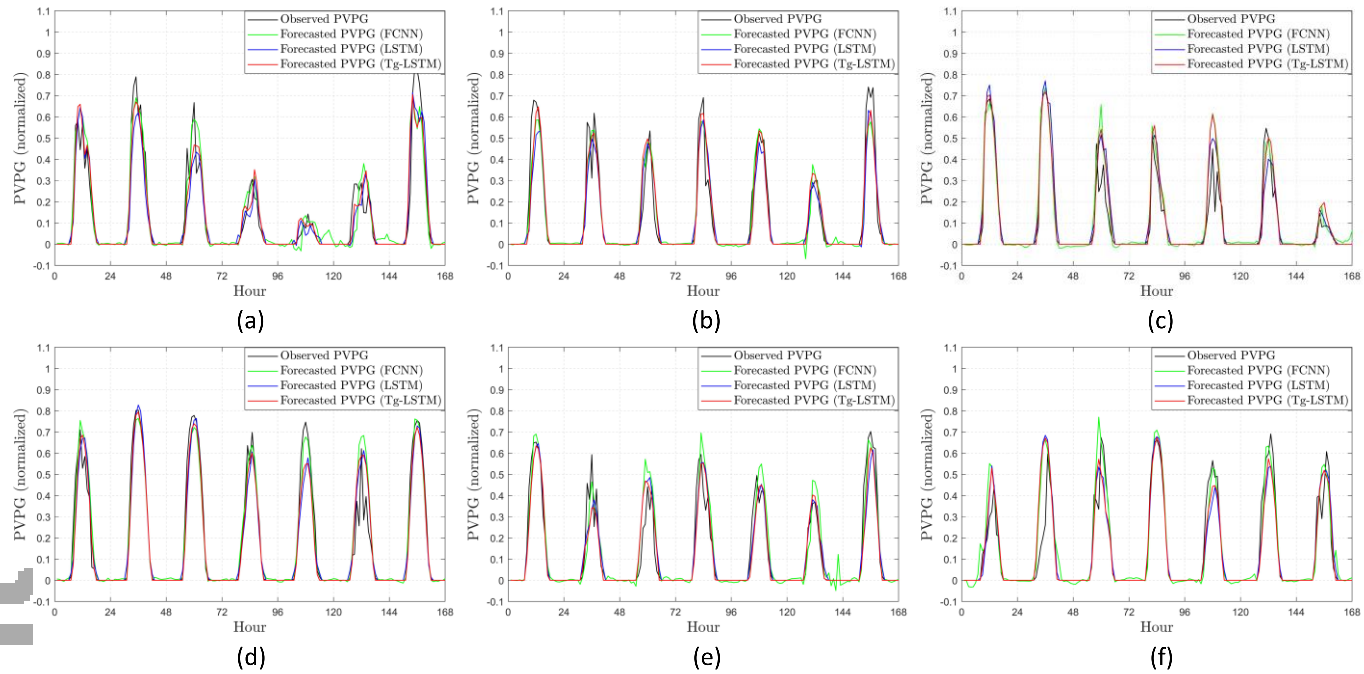


Fig. 5: Results of PVPG forecasting based on different models. (a) PV plant #1 - Case #1; (b) PV plant #1 - Case #2; (c) PV plant #1 - Case #3; (d) PV plant #2 - Case #1; (e) PV plant #2 - Case #2; (f) PV plant #2 - Case #3.

high accuracy with sparse data. The results illustrate that the Tg-LSTM model is more suitable for PVPG forecasting with sparse data than the standard LSTM model.

### *3.3 Tg-LSTM based PVPG forecasting*

The performances of hourly day-ahead PVPG forecasting at different times for two PV plants are also evaluated. After training the Tg-LSTM model for multiple times, PVPG forecasting models are established. The same hyper-parameters are adopted for both LSTM and Tg-LSTM models. The Tg-LSTM model is compared with the standard LSTM and fully connected neural network (FCNN) [1] in this case.

To visually display the forecasting results, the hourly day-ahead PVPG forecasting values of seven continuous days of each month in the testing dataset (3 months from April to June) for both PV plants are presented in Fig. 5. From the results, it can be seen that all three compared models can accomplish the task of PVPG forecasting with acceptable accuracies. The forecasted PVPG curves are in line with the variations of observed PVPG, in general. The result obtained by the Tg-LSTM model, however, is smoother and better than the results of the other two models to some extent. It is noted that some detailed variations of PVPG are not forecasted well by all methods, since the adopted weather data are forecasted values, which may result in certain difficulty in the PVPG forecasting. In addition, some physically unreasonable forecasts (e.g., negative power generation and positive power generation at midnight) occurred by using conventional FCNN; whereas, they are significantly restricted by the Tg-LSTM model due to the contributions made by the integrated constraints.

Table 1: Evaluation of PVPG forecasting by using different models in different cases.

| PV plant | Case index | Models | Evaluation metrics | | |
|---|---|---|---|---|---|
| | | | $MAE^{\times 10^{-2}}$ | $MSE^{\times 10^{-3}}$ | $R^2$ |
| Plant #1 | Case #1 | FCNN | 3.72 | 4.83 | 0.890 |
| | | LSTM | 3.82 | 5.35 | 0.878 |
| | | Tg-LSTM | **3.37** | **4.60** | **0.895** |
| | Case #2 | FCNN | 3.43 | 4.41 | 0.898 |
| | | LSTM | 3.39 | 4.92 | 0.886 |
| | | Tg-LSTM | **3.10** | **4.06** | **0.906** |
| | Case #3 | FCNN | 3.09 | 4.67 | 0.863 |
| | | LSTM | 2.98 | 4.29 | 0.874 |
| | | Tg-LSTM | **2.62** | **4.20** | **0.877** |
| Plant #2 | Case #1 | FCNN | 3.27 | 4.53 | 0.937 |
| | | LSTM | 3.78 | 5.26 | 0.926 |
| | | Tg-LSTM | **3.24** | **4.37** | **0.939** |
| | Case #2 | FCNN | 4.12 | 5.14 | 0.870 |
| | | LSTM | 3.40 | 4.68 | 0.882 |
| | | Tg-LSTM | **3.25** | **4.52** | **0.886** |
| | Case #3 | FCNN | 4.09 | 7.40 | 0.829 |
| | | LSTM | 3.92 | 7.38 | 0.829 |
| | | Tg-LSTM | **3.70** | **6.82** | **0.842** |

The evaluation of PVPG forecasting of the above cases is presented in Table 1. The best results are marked in bold. The results are also in accordance with the previous analysis. The proposed Tg-LSTM model can achieve better forecasting performance with lower values of MAE and MSE, and higher values of $R^2$ score in the comparison in each case, which verified the superiority of the Tg-LSTM model over other compared models.

## 4. CONCLUSION

Incorporating domain knowledge of PV, a theory-guided LSTM framework was proposed to address the hourly day-ahead PVPG forecasting problem. From the results, it can be concluded that the proposed Tg-LSTM model is more robust against PVPG forecasting and more suitable for the small-scale dataset based PVPG forecasting problem than the standard LSTM model. It also demonstrated superior performance with higher accuracy of hourly day-ahead PVPG forecasting compared to conventional machine learning methods. Through Tg-LSTM, deep learning is not only driven by data, but also by domain knowledge, such as physical laws and engineering controls of a specific problem, which can assist the model to obtain better accuracy, robustness, and interpretability.


## ACKNOWLEDGEMENT

The research is partially supported with special funds from the Peng Cheng Laboratory and start-up funds from the Southern University of Science and Technology (SUSTech).


## REFERENCE


[1] J. Zheng, H. Zhang, Y. Dai, B. Wang, T. Zheng, Q. Liao, Y. Liang, F. Zhang, X. Song, Time series prediction for output of multi-region solar power plants, Applied Energy 2020; 257: 114001.

[2] S. Lin, C. Li, F. Xu, D. Liu, J. Liu, Risk identification and analysis for new energy power system in china based on d numbers and decision-making trial and evaluation laboratory (dematel), Journal of Cleaner Production 2018; 180: 81–96.

[3] A. Strzalka, N. Alam, E. Duminil, V. Coors, U. Eicker, Large scale integration of photovoltaics in cities, Applied Energy 2012; 93: 413–421.

[4] Y. S. Manjili, R. Vega, M. M. Jamshidi, Data-analytic-based adaptive solar energy forecasting framework, IEEE Systems Journal 2018; 12 (1): 285–296.

[5] A. Gensler, J. Henze, B. Sick, N. Raabe, Deep learning for solar power forecasting - an approach using auto encoder and lstm neural networks, in: IEEE International Conference on Systems, Man, and Cybernetics, 2016; pp. 2858–2865.

[6] N. Wang, D. Zhang, H. Chang, H. Li, Deep learning of subsurface flow via theory-guided neural network, Journal of Hydrology 2020; 584: 124700.

[7] L. von Rueden, S. Mayer, K. Beckh, B. Georgiev, S. Giesselbach, R. Heese, B. Kirsch, J. Pfrommer, A. Pick, R. Ramamurthy, M. Walczak, J. Garcke, C. Bauckhage, J. Schuecker, Informed machine learning - a taxonomy and survey of integrating knowledge into learning systems 2019; arXiv:1903.12394.

[8] X. Luo, X. Zhu, E. G. Lim, A parametric bootstrap algorithm for cluster number determination of load pattern categorization, Energy 2019; 180: 50–60.

[9] T. Hong, P. Pinson, S. Fan, H. Zareipour, A. Troccoli, R. J. Hyndman, Probabilistic energy forecasting: Global energy forecasting competition 2014 and beyond, International Journal of Forecasting 2016; 32 (3): 896–913.

[10] M. Abuella, B. Chowdhury, Solar power forecasting using artificial neural networks, in: North American Power Symposium 2015, pp. 1–5.